Cerebral Cortex September 2012;22:2171–2181
doi:10.1093/cercor/bhr304
Advance Access publication November 2, 2011

# Loss of Visually Driven Synaptic Responses in Layer 4 Regular-Spiking Neurons of Rat Visual Cortex in Absence of Competing Inputs

Giuliano Iurilli, Fabio Benfenati and Paolo Medini

Neuroscience and Brain Technologies Department, Italian Institute of Technology, Via Morego 30, 16163 Genova, Italy

Address correspondence to Paolo Medini. Email: paolo.medini@iit.it.

**Monocular deprivation (MD) during development shifts the ocular preference of primary visual cortex (V1) neurons by depressing closed-eye responses and potentiating open-eye responses. As these 2 processes are temporally and mechanistically distinct, we tested whether loss of responsiveness occurs also in absence of competing inputs. We thus compared the effects of long-term MD in layer 4 regular-spiking pyramidal neurons (L4Ns) of binocular and monocular V1 (bV1 and mV1) with whole-cell recordings. In bV1, input depression was larger than potentiation, and the ocular dominance shift was larger for spike outputs. MD—but not retinal inactivation with tetrodotoxin—caused a comparable loss of synaptic and spike responsiveness in mV1, which is innervated only by the deprived eye. Conversely, brief MD depressed synaptic responses only in bV1. MD-driven depression in mV1 was accompanied by a proportional reduction of visual thalamic inputs, as assessed upon pharmacological silencing of intracortical transmission. Finally, sub- and suprathreshold responsiveness was similarly degraded in L4Ns of bV1 upon complete deprivation of patterned vision through a binocular deprivation period of comparable length. Thus, loss of synaptic inputs from the deprived eye occurs also in absence of competition in the main thalamorecipient lamina, albeit at a slower pace.**

**Keywords:** in vivo whole cell, layer specificity, ocular dominance plasticity, primary visual cortex

## Introduction

Monocular deprivation (MD) during the critical period is widely used in rodents to study the cellular and molecular basis of experience-dependent plasticity of cortical circuits. MD causes an ocular preference shift in binocular primary visual cortex (bV1) neurons that is due to the combined effect of depression of the deprived-eye inputs and potentiation of open-eye responses (Mioche and Singer 1989; Frenkel and Bear 2004; Mrsic-Flogel et al. 2007; Restani et al. 2009). Loss of responsiveness to deprived eye is responsible for amblyopia and is thought to be the outcome of a process of activity-dependent competition between the synaptic inputs coming from the 2 eyes (Wiesel and Hubel 1965; Gordon and Stryker 1996), resulting in reduced glutamatergic inputs to the main thalamorecipient lamina, layer 4 (Heynen et al. 2003; Yoon et al. 2009). The weaker effect of monocular inactivation (MI) with intravitreal tetrodotoxin (TTX) on the ocular preference shift of bV1 neurons compared with lid suture (Rittenhouse et al. 1999) indicates that depression of closed-eye responses occurs via homosynaptic long term depression (LTD). Moreover, loss of responsiveness to the deprived eye temporally precedes (Mioche and Singer 1989; Frenkel and Bear 2004) and is mechanistically different from potentiation of open-eye responses (Heynen et al. 2003; Kaneko et al. 2008), indicating that the 2 plastic processes are at least partially independent. This, together with the role of homosynaptic LTD in MD-driven loss of responsiveness, suggests that depression of visual responses could occur independently of the presence of competing inputs. This possibility is also suggested by the observation that the number of unresponsive units is abnormally high in kittens subjected to binocular deprivation (BD) (Wiesel and Hubel 1965) or to a brief period of dark rearing (Freeman et al. 1981). However, extracellular recordings along the whole cortical depth in juvenile mice showed only a slight decrease of spiking responses (Gordon and Stryker 1996) and of visually evoked potential (VEP) amplitude (Frenkel and Bear 2004) in mouse bV1 upon 3–4 days of BD. Conversely, a more prolonged period (2 weeks) of BD reduces visual responsiveness in bV1 as assessed by intrinsic signal imaging (ISI) (Faguet et al. 2009). Another well-suited model to study the synaptic effects of MD in the absence of competing inputs is the relatively large monocular field of primary visual cortex (V1) in rodents, which is innervated only by thalamic inputs driven by the contralateral eye. The effects of MD in monocular primary visual cortex (mV1) remain unclear. In rodents, flavoprotein imaging (Tohmi et al. 2006), functional anatomy with c-fos staining (Pham et al. 2004), and layer 4 VEPs (Smith et al. 2009) failed to find consistent effects of MD in mV1. On the other hand, ISI (Kaneko et al. 2008; Faguet et al. 2009), epidural VEPs (Heynen et al. 2003), as well as extracellular unit recording (Spolidoro et al. 2011) reported that MD significantly degrades responsiveness in mV1 of juvenile mice. Conversely, a two-photon calcium imaging study in supragranular layers revealed a significant increase in responsiveness of mouse V1 upon both MD in mV1 and BD in bV1 (Mrsic-Flogel et al. 2007), raising the possibility of layer-specific effects. Here, we addressed the role of competition in MD-driven loss of responsiveness by comparing the sub- and suprathreshold effects of MD between mV1 and bV1 in populations of identified cortical neurons. At this purpose, we did ISI-targeted in vivo whole-cell recordings from pyramidal neurons of layer 4, which is the cortical lamina where the synaptic changes are primarily expressed upon critical period MD (Coleman et al. 2010; Khibnik et al. 2010).

## Materials and Methods

### *Intrinsic Signal Imaging*

All animal procedures have been done in agreement with the regulations for animal welfare from the Italian Ministry of Health. Long–Evans rats (aged P30–P32) were anesthetized with urethane (1.6 g/kg, intraperitoneal (i.p.)). Dexamethazone (0.01 mg/kg, i.p.) was injected to prevent cortical and mucosal edema. Oxygen was administered to the animal through a nose cannula, and body temperature was maintained at 37 °C through a thermostatic blanket. Corneal and pinch reflexes, electrocardiogram, and breathing rate were

continuously monitored during the experiment. Rats were mounted on a stereotaxic apparatus, and a region of skull lying above V1 of about 4 × 4 mm was thinned until the underlying vasculature was clearly visible. An imaging chamber made with acrylic cement was built on the skull and filled with saline warmed at 37 °C. A vasculature ("green") image was acquired under 540 nm illumination before starting the imaging session. During ISI, the cortex was illuminated with monochromatic light of 630 nm wavelength. Images were acquired using a cooled 50 Hz CCD camera connected with a frame grabber (Imager 3001; Optical Imaging Inc, Germantown, NY), defocused approximately 500–600 μm below the pial surface. Data frame duration was 200 ms, and a spatial binning of 3 × 3 was applied over the images, which were 4.5 × 4.5 mm, with a pixel resolution of about 25 μm.

*Visual Stimulation during ISI*

Eye bulbs were kept fixed with metal rings adjusted so that the eye pupils projected at approximately 55–57° with respect to the vertical meridian. Corneas were protected with artificial tears. Squared spots of 20° × 20° were randomly projected in 9 different positions and presented to the contralateral eye. A craniotomy was opened in correspondence to the spot position flanking the vertical meridian (between 5° and 25° of eccentricity) and at 20° of elevation for recordings in bV1 and at 50–55° of eccentricity for recordings in mV1. The spots displayed squared drifting gratings (duration: 8 s, spatial frequency: 0.05 cycles/deg, speed: 2 cycles/s, contrast: 90%, mean grating luminance: 19 cd/m$^2$). Stimulus orientation was randomly alternated during the 8 s of stimulation (every 45°, every seconds), and stimuli were randomly interleaved with a full-field blank screen whose luminance was equal to the mean luminances of the grating (K0 blank). This same background surrounded the stimulus spot. Stimuli were displayed at 25 cm from the animal's eyes on a Sony G520 cathode ray tube 22″ monitor. Ten blank "first frames" were collected before stimulus onset.

*Image Analysis*

All image frames obtained during stimulus presentation were divided by the average image of the first 10 frames acquired just before stimulus presentation. The relative decrease of reflectance, averaged over the stimulus presentation period, was then outlined. The spot area was taken as the image area where the visually evoked decrease in reflectance was higher than 50% of the peak decrease. This region was then overlaid with the vasculature green image (see Fig. 4*A*).

***Visual Deprivations and Eye Protection***

Rats were anesthetized with avertin (tribromoethanol solution; 1 mL/hg animal weight) and placed on a thermostatic blanket. Eyelids were suture-closed with 6-0 surgical wire (Ethicon) under a surgical microscope with 3 mattress stitches. Control littermates were also anesthetized. Ophthalmologic ointment containing hydrocortisone and gentamicin was applied during surgery. Animals showing any reopening during the deprivation period or with corneal opacities (revealed at ophtalmoscopic examination on the day of recording) were discarded. During experiments, artificial tears were used to prevent corneal dehydratation and ophthalmological examination of both the cornea and the visible part of the lens through the pupils was performed to exclude opacities of the eye optics.

***Intravitreal Blockade of Retinal Activity***

To block retinal ganglion cells spiking, we slowly injected (injection time: 1 min) 1 μL of 3 mM TTX dissolved in 0.025 M citrate buffer (pH 4.5) by means of a pressure-controlled injector (Caleo et al. 1999; Frenkel and Bear 2004; Maffei and Turrigiano 2008). Injections were repeated every 24 h and were done just behind the "ora serrata" in correspondence of the temporal and rostral part of the retina so to minimize damage to nasal retinal cells, which are stimulated by the temporal monocular visual field. Retinal blockade was controlled at least twice per day by checking pupil dilation and lack of pupil constriction upon direct retinal illumination. At the end of the series of intravitreal TTX injections, animals were subjected to eyelid suturing of the injected eye for 48 h to allow TTX washout in the absence of patterned vision (Caleo et al. 1999; Frenkel and Bear 2004).

***Extracellular Mapping and VEPs***

A 400- to 500-μm wide craniotomy was opened over the ISI spot of interest, and the underlying dura was carefully cut and lifted apart. Receptive field (RF) position and binocularity within the craniotomy were checked with 1 MΩ glass pipettes filled with normal rat Ringer's solution (in mM: 135 NaCl, 5.4 KCl, 1.8 $CaCl_2$, and 1 $MgCl_2$). The signal was band filtered (500 Hz–5 kHz), amplified (×10 000), and the action potential (AP) activity of neurons was visualized and heard using an AP discriminator (npi instruments, Germany). The pupils, the vertical and horizontal meridians, were projected onto a circular screen put at 20 cm from the animal's eyes. RF positions were plotted using light bars moved manually through a back projector. For VEP recordings, the signal was band filtered at 0.1–110 Hz. Visual stimulation was done with squared gratings alternating in counter phase displayed at 20 cm from the animal eye, taking care that the screen was centered on the spot used during the ISI session. Stimulation parameters were as follows: spatial frequency 0.05 C/deg, temporal frequency: 0.5 Hz, contrast: 90%, and mean luminance: 20 cd/m$^2$.

***Blockade of Intracortical Synaptic Transmission***

To isolate thalamocortical inputs onto layer 4 regular-spiking pyramidal neurons (L4Ns), we followed the protocol of Liu et al. (2007) applied in mouse V1 for the first time by Khibnik et al. (2010). About 50–100 nL of cocktail solution containing 1 mM of muscimol and 1.5 mM of SCH50911 (muscimol+) was slowly injected within layer 4 at the center of the craniotomy through a pressure injection system. VEP recordings were continuously monitored, and in vivo whole-cell recordings began only when the VEP signal did not diminish further after muscimol+ injection (which occurred after 20–30 min). Patching was done within 1 h, a time window consistent with the reported duration of muscimol+ effects (Liu et al. 2007; Khibnik et al. 2010). At the end of the intracellular recordings, we always monitored that the VEP signal had not recovered. In a subset of muscimol+-injected animals, 1 μL of 4 mM muscimol was stereotaxically injected into the lateral geniculate nucleus, and the VEP signal was recorded from V1 after 20 min ($n$ = 2; data not shown). This manipulation removed the residual VEP signal (no signal larger than baseline + 1 standard deviation [SD] was evoked), confirming that the latter merely reflected thalamocortical inputs (see also Khibnik et al. 2010).

***In Vivo Whole-Cell Recordings***

Five to nine mega ohms borosilicate patch pipettes filled with intracellular solution (in mM: 135 K gluconate, 10 4-(2-hydroxyethyl)-1-piperazineethanesulfonic acid, 10 Na phosphocreatine, 4 KCl, 4 ATP-Mg, 0.3 GTP, pH 7.2, 3 mg/mL biocytin, osmolarity 291 mOsm) were lowered perpendicularly to the pia applying approximately 300 mmHg of positive pressure until the layer of interest was reached. At that point, positive pressure was lowered to 30 mmHg, and cells were searched for in voltage clamp mode. On approaching a cell, pressure was relieved and light suction was applied to allow gigaseal formation. After capacitance compensation, a ramp of negative pressure usually led to whole-cell configuration. Recordings were performed with an EPC10plus (HEKA, Germany) operated in bridge mode. The membrane potential ($V_m$) signal was digitized at 20 kHz and acquired using the program Patchmaster (Heka Elektronic, Germany). Access resistance was repeatedly monitored, compensated for and ranged between 10 and 100 MΩ. Seal resistance was higher than 2 GΩ, and spike height and overall $V_m$ were stable throughout recordings. No holding current was used. Recording durations ranged from 20 min to 2 h.

*Cell Characterization*

The resting $V_m$ of neurons was measured as the modal value of the most negative peak in the $V_m$ distribution during spontaneous activity ($V_m$ during Down states). AP threshold was measured at the peak of the second derivative of the $V_m$ trace (Wilent and Contreras 2005). Input

resistance was measured by the steady voltage response to 300 ms duration hyperpolarizing current pulses (−100 pA). The firing pattern was obtained by measuring the $V_m$ response to 1 s current injections, and the AP adaptation characteristics were computed as the ratio between the average of the first and the last 3 interspike intervals upon a current injection level causing at least 10 APs (Margrie et al. 2003). The AP width was measured as the width of the AP at half-maximal amplitude measured from threshold to peak (see, e.g., Fig. 1*B*).

*Visual Stimulation*

The screen was positioned at 20 cm from the rat's eyes and centered on the spot positions used during the ISI session. Three degrees wide moving light bars (luminance: 20 cd/m$^2$, background luminance: 3 cd/m$^2$, angular speed: 45–55 deg/s) of various orientations (every 45°) were separately presented to the 2 eyes by means of computer-controlled custom-made mechanical eye shutters. A period of 4 s between the end of one stimulus presentation and the beginning of the next one was set to prevent adaptation of responsiveness.

*Analysis of Visual Responses*

Data were analyzed using a custom-made software written in IgorPro (Wavemetrics). For the analysis of subthreshold responses, APs were truncated using linear interpolation, and sweeps were averaged over 20 presentations. Cells were first screened for their preferred orientation using light bars moving in various orientations (every 45°). To compare the response strength of the 2 eyes, only sub- and suprathreshold responses in the preferred orientation (and direction) were considered. "Postsynaptic potential (PSP) amplitude" was computed with respect to the mean $V_m$ during the interstimulus period. To compute the amplitude of visually evoked "AP responses," mean spontaneous AP rates were subtracted to take into account differences of this parameter among cells. To compute peristimulus time histograms (PSTHs) of AP counts, 50 ms binning was applied. Suprathreshold "RF size" was measured as the amplitude in visual degrees of the region of visual space whose stimulation evoked an AP rate higher than the baseline AP rate plus 2.5 SDs (Pizzorusso et al. 2002). Similarly, subthreshold RF size was measured from the PSP response as the angular amplitude of the region of visual space whose stimulation evoked an averaged $V_m$ signal that was higher than the average baseline $V_m$ plus 2.5 SDs. Baseline measures were taken from the PSP response or from the PSTHs of AP counts during the interstimulus interval. "Reliability" of suprathreshold visual responses was quantified by computing the coefficient of variation of the total number of APs fired inside the cell's RF on a single trial basis. To quantify "ocular preference," we computed an ocular dominance index (ODI) for every cells defined as $(C - I)/(C + I)$, where $C$ and $I$ are the amplitudes of the peak PSP (or AP) responses for the contralateral and ipsilateral eye, respectively.

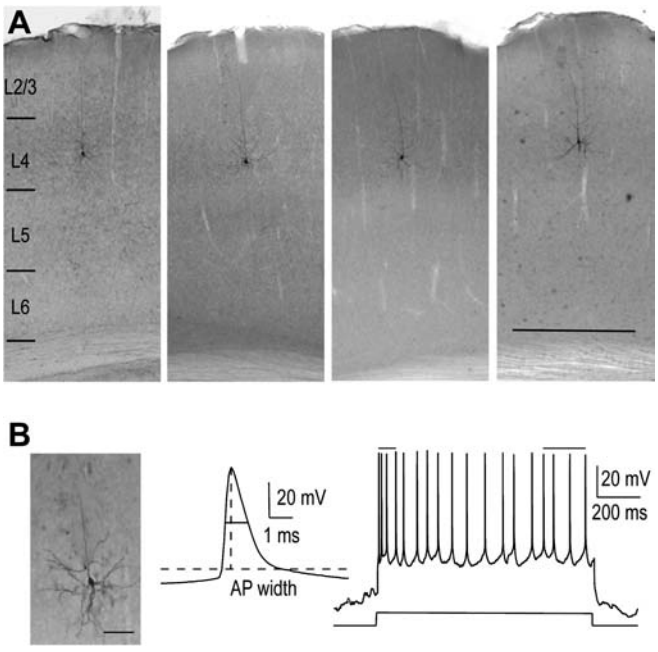


**Figure 1.** ISI-targeted in vivo whole-cell recordings from regular spiking layer 4 pyramids. (*A*) Histochemical labeling of byocitin-filled L4Ns recorded in vivo by ISI-targeted whole-cell recordings. Sections are counterstained for cytochrome C to reveal layer 4. Pictures are montages of microphotographs taken from adjacent sections to show the untufted apical dendrite. Bar: 500 μm. (*B*) Recorded cells were regular spiking, as defined by their "broad" APs (example of AP width measurement in the middle trace) and by their adapting firing pattern in response to 1 s current injection (right). The adaptation ratio was calculated as the ratio between the mean of the first and the last 3 interspike intervals (top lines) fired in response to a current injection able to evoke at least 10 APs. Bar: 50 μm.

***Histochemical Staining and Neuronal Identification***

At the end of the recording sessions, animals were deeply anesthetized with urethane (i.p.) and fixed through the heart with 60 mL of cold phosphate buffer 0.1 M, followed by 120 mL of freshly dissolved 4% paraformaldehyde in 0.1 M phosphate buffer. Brains were postfixed in paraformaldehyde 4% in 0.1 M phosphate buffer overnight. Coronal sections (100 μm thick) were cut using a vibratome, stained for biocytin to reveal recorded neurons, and counterstained for cytochrome oxidase to reveal layer 4 (Tsiola et al. 2003). Sections were then mounted and coverslipped with Mowiol, and cell identity was controlled under a brightfield microscope.

***Statistical Analysis***

Normality was tested using both a Kolmogorov–Smirnov test and a Shapiro–Wilk test. For normally distributed data, means ± standard error of the mean are reported, otherwise medians are reported. Box plots represent the extremes (crosses), the 5–95 percentile (outer segments) and the 25–75 percentile (box); the line inside the box is the median, and the square is the mean. The following comparisons have been done: normally distributed data were compared with *t*-tests (when unpaired) or with paired *t*-tests (when paired); nonnormally distributed data were compared with Mann–Whitney rank sum test for unpaired comparisons. Statistical comparisons among more than 2 groups have been done with one-way analysis of variance (ANOVA), followed by the Tukey's multiple comparison tests for normally distributed data and with ANOVA on ranks followed by the Dunn's multiple comparison test for normally distributed data.

## Results

### *Intrinsic Signal–Targeted In Vivo Whole-Cell Recordings from Regular Spiking Layer 4 Pyramids in Rat V1*

ISI through the thinned skull was used to target in vivo whole-cell recordings (see Materials and Methods). This approach allowed us to open small craniotomies to improve the mechanical stability of the recordings and reduce variations of those RF properties that depend on eccentricity such as angular size and ocular preference (Gordon and Stryker 1996). Subsequent intracellular recordings were targeted to layer 4 (micromanipulator nominal depths: 500–730 μm). Recorded byocitin-filled cells were recovered by histochemical staining, and layer 4 was revealed using cytochrome oxidase staining. As shown in the examples of Figure 1, the cells we recovered were layer 4 pyramids, without a tufted apical dendrite, in agreement with the observation that spiny stellate cells are rare in rat V1 (Peters et al. 1985). The firing characteristics of all neurons (see Materials and Methods) were typical of regular-spiking cells, as based on their firing rates (see Table 1), spike duration (AP half width measured from threshold: 1.06 ± 0.03 ms), shape (lack of fast afterhyperpolarization), and spike adaptation ratio (3.08 ± 0.26) (see Fig. 1*B*; Chadderton et al. 2009; Gentet et al. 2010). As reported by other groups

**Table 1**
Effects of MD on spontaneous activity of L4Ns in bV1 and mV1

| L4Ns | bV1 | | mV1 | |
|---|---|---|---|---|
| | Normal | MD P20–P30 | Normal | MD P20–P30 |
| Resting (down) $V_m$ (mV) | −68.7 ± 1.3 | −67.8 ± 1.4 | −69.9 ± 1.6 | −69.5 ± 1.4 |
| Spontaneous APs (APs/s) | 0.53 ± 0.10 | 0.90 ± 0.14 | 0.58 ± 0.18 | 0.54 ± 0.16 |
| Input resistance (MΩ) | 123.9 ± 8.1 | 118.2 ± 9.4 | 93.9 ± 12.6 | 100.2 ± 11.1 |
| AP threshold (mV) | −35.5 ± 0.8 | −36.4 ± 0.8 | −36.0 ± 1.0 | −36.2 ± 1.0 |

Note: Means ± standard error of the mean are reported.

(e.g., Brecht and Sakmann 2002; Brecht et al. 2003; Chadderton et al. 2009; Constantinople and Bruno 2011), the in vivo blind whole-cell approach from young adult animals yielded only very rarely recordings from interneurons. Indeed, we only occasionally recorded from aspiny, nonpyramidal cells, with the firing pattern, frequency, and AP shape typical of fast-spiking interneurons ($n = 6$). These latter cells were excluded from the current analysis.

### *The Ocular Dominance Shift Caused by MD in L4Ns Was Larger for AP Responses*

We first evaluated the sub- and suprathreshold effects of long-term MD (P20–P30) in L4Ns of bV1 in pigmented rats. For these experiments, we targeted the central upper binocular visual field of area V1 by means of ISI (see Materials and Methods). We measured the peak amplitude of sub- and suprathreshold visual responses of L4Ns with respect to the interstimulus period upon stimulation with light bars moving in the cell preferred orientation (see Materials and Methods). The examples of Figure 2*A* show that, in normal rats, the contralateral bias of visual responses was sharper for AP responses compared with PSPs. We computed an ODI for every cell defined as $(C - I)/(C + I)$, where $C$ and $I$ are the amplitudes of the PSP (or AP) responses through contralateral and ipsilateral eye stimulation, respectively. This index varies from +1 to −1 for cells driven solely by the contralateral or ipsilateral eye, respectively, and is 0 for perfectly binocular cells. At population level, the ODI of L4Ns was positive as cells were dominated by contralateral eye inputs and was higher for AP responses compared with PSPs (Fig. 2*B*; 18 rats, 24 cells; paired *t*-test, $P < 0.05$). Upon long-term MD, cells shifted their ocular dominance in favor of the open eye, as shown by the examples of Figure 2*A* and by the decrease of their PSP-ODI (Fig. 2*B*, dashed boxes; normal vs. MD rats: 0.21 ± 0.04 vs. –0.13 ± 0.05; *t*-test, $P < 0.001$). Thus, the ocular dominance shift caused by MD was larger at suprathreshold level (Fig. 2*B*; MD rats: 18 rats, 24 cells; AP-ODIs for normals and MD rats: 0.38 ± 0.08 vs. –0.47 ± 0.09, *t*-test, $P < 0.001$). The analysis of the cumulative frequency distributions of AP-ODIs and PSP-ODIs confirmed that 1) the contralateral bias of visual responses is more pronounced at suprathreshold level in normal rats and 2) MD effects on the ocular preference shift are larger for AP responses compared with PSPs (Fig. 2*C*; Kolmogorov–Smirnov statistics, $P < 0.01$).

### *Depression of Deprived-Eye Synaptic Responses Was Larger Compared with Potentiation of Open-Eye Responses*

We investigated to which extent the ocular preference shift caused by MD in bV1 was due to depression of synaptic inputs

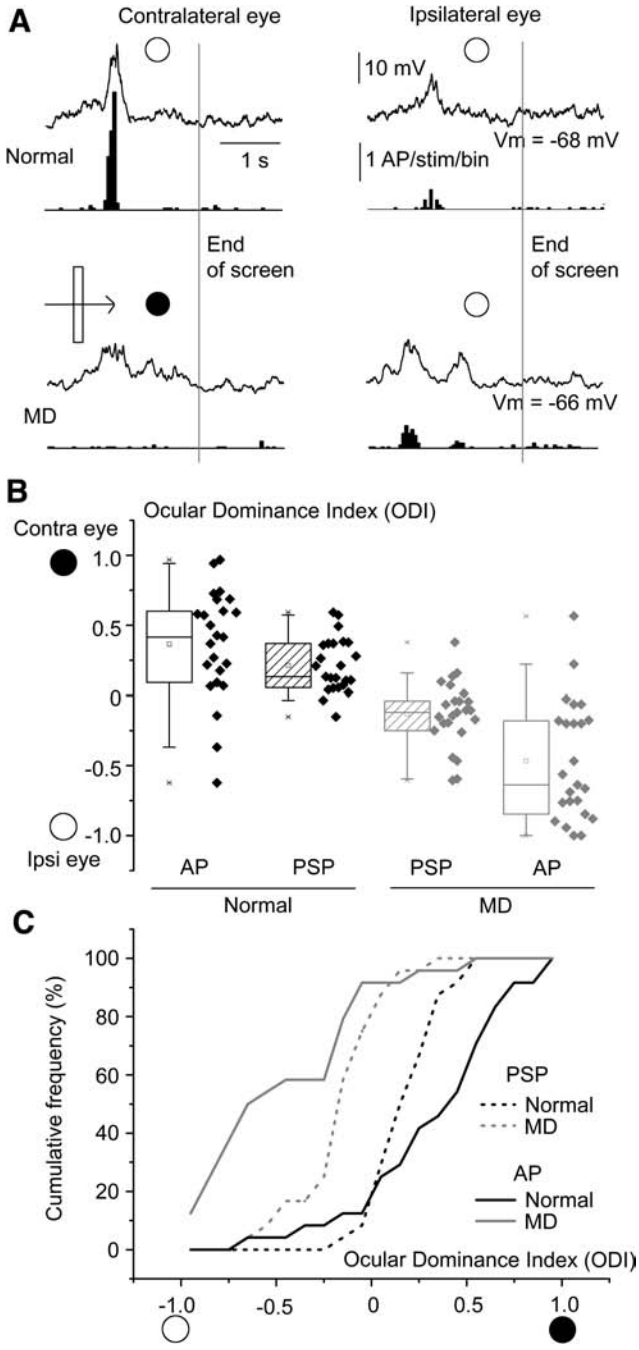


**Figure 2.** The shift of ocular preference caused by MD in L4Ns was larger at suprathreshold level. (*A*) Example of PSP (traces) and AP (PSTHs) responses of L4Ns in bV1 to contralateral and ipsilateral eye stimulation with optimally oriented moving bars in a normal rat (top) and upon long-term MD (bottom). Traces and PSTHs have been obtained after averaging the responses to 20 stimulus passages. The light bar starts moving at the sweep beginning and reaches the end of the screen in correspondence of the gray vertical lines. (*B*) Box plots of sub- and suprathreshold ODIs of L4Ns recorded in normal (black) and MD (gray) rats. Note that, in both groups, the ocular preference for the dominant eye (the contra- and ipsilateral in normals and MD rats, respectively) is sharper at suprathreshold level. MD effects are thus more pronounced at suprathreshold level (paired *t*-tests, $P < 0.05$). (*C*) Plot showing the cumulative frequency distributions of the ODIs at PSP level (dashed lines) and AP level (continuous lines) in normal (black) and MD (gray) rats. This confirms that, in normal rats, the contralateral bias of visual responses is sharper at suprathreshold level and that the effects of MD on the ocular preference shift are larger at suprathreshold level (Kolmogorov–Smirnov test, $P < 0.01$).

coming from the deprived eye or to potentiation of those driven by the open eye. The example shown in Figure 2*A* suggests that loss of responsiveness to the closed eye plays a major role. Quantification of the amplitudes of sub- and suprathreshold responses of L4Ns upon independent stimulation of the 2 eyes confirmed a significant depression of deprived-eye PSP responses (Fig. 3*A*; 17.1 ± 1.1 vs. 10.7 ± 0.9 mV for normal and MD rats, respectively; *t*-test, $P < 0.001$), whereas potentiation of PSPs driven by the open eye was less pronounced and did not reach significance (Fig. 3*A*; 11.2 ± 1.0 vs. 13.9 ± 1.1 mV for normal and MD rats, respectively; *t*-test, $P = 0.07$). At suprathreshold level, MD caused a significant depression of AP responses driven by the closed eye (Fig. 3*B*; medians: 0.94 vs. 0.35 APs/stimulus/bin for normal and MD rats, respectively; Mann–Whitney rank sum test, $P < 0.001$). The increase in the amplitude of visual responses driven by the left open eye became significant when AP responses were compared (Fig. 3*B*; medians: 0.44 vs. 0.75 APs/stimulus/bin for normal and MD rats, respectively; Mann–Whitney rank sum test, $P < 0.01$). We finally analyzed whether sub- and suprathreshold spontaneous activity was altered by MD with respect to control animals in bV1 (see Table 1). We failed to find differences in resting mean $V_m$ values, spontaneous firing rates, and cell excitability, as expressed by the cell input resistance and AP threshold measurements (*t*-tests, statistical significance: $P > 0.05$).

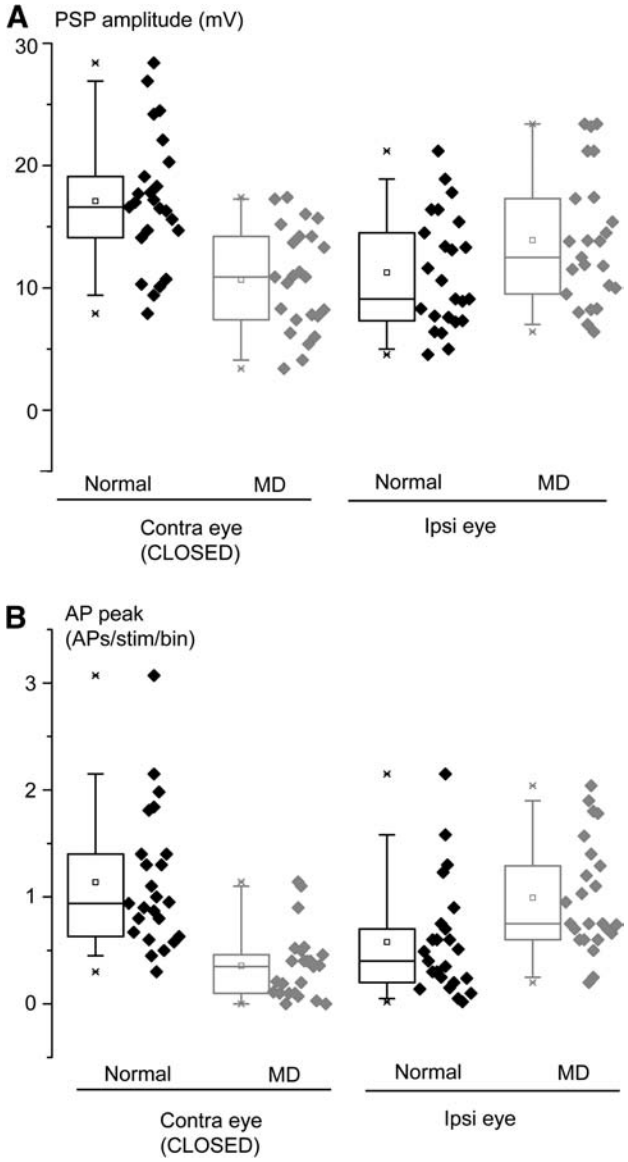


**Figure 3.** MD shifted the ocular preference of L4Ns mostly by depressing closed-eye responses. Box plots showing the amplitude of subthreshold (*A*) and suprathreshold (*B*) responses of L4Ns to independent stimulation of the 2 eyes in normal (black) and MD (gray) rats. (*A*) Loss of synaptic responsiveness to the contralateral deprived eye was significant, while potentiation of open-eye responses only approached significance (*t*-tests, $P < 0.001$ and $P = 0.07$, respectively). (*B*) In the case of suprathreshold responses, both depression of the closed contralateral eye responses and potentiation of the open ipsilateral eye responses were significant (Mann–Whitney rank sum tests, $P < 0.001$ and $P < 0.01$, respectively).

Thus, loss of synaptic responsiveness to the deprived eye was larger compared with potentiation of open-eye inputs. Both effects, became however significant at suprathreshold level.

### *MD Reduced Sub- and Suprathreshold Responses of L4Ns in mV1*

mV1 was identified by means of ISI through the thinned skull. All recordings were done in an ISI spot located at 50–55° of eccentricity (Fig. 4*A*) and confirmed by subsequent extracellular RF mapping and VEP recordings within the corresponding craniotomy. As shown in the examples and in the grand averages of the VEP recordings (black trace of Fig. 4*B*), responses to squared gratings alternating in counterphase were obtained only through contralateral eye stimulation. No significant VEP response was found upon stimulation of the ipsilateral eye (gray traces in Fig. 4*B*). The somata of recorded L4Ns were located at a mean distance of 2.98 ± 0.09 mm from the midline, consistent with the position of mV1 in the rat brain (Zilles et al. 1984). As shown in the examples of Figure 4*C*, subthreshold visual responses recorded from MD rats (11 rats, 19 cells) in mV1 were smaller compared with controls (12 rats, 19 cells). Indeed, we found a significant decrease in the amplitude of visually driven PSPs upon MD in L4Ns of mV1, which was comparable to that observed in bV1 (Fig. 4*D*, upper panel; 17.8 ± 1.5 vs. 10.1 ± 1.0 mV in normal and MD rats, respectively; *t*-test, $P < 0.001$). A similar result was found for the peak amplitude of AP responses, corrected for the spontaneous activity (examples of Fig. 4*C* and middle panel of Fig. 4*D*; medians: 0.71 vs. 0.30 APs/stimulus/bin for normal and MD rats, respectively; Mann–Whitney rank sum test, $P = 0.01$). We also quantified the reliability of visually driven firing by computing the coefficient of variation of AP counts (fired inside the cell RF) on a single-trial basis. MD significantly reduced reliability of AP responses as expressed by a statistically significant increase of the coefficient of variation (see examples of raster plots of Fig. 4*C*, and Fig. 4*D*, lower panel; medians: 0.65 vs. 1.41 for coefficient of variation of normal and MD rats; Mann–Whitney rank sum test, $P < 0.05$). We finally checked whether the angular size of RFs was affected by MD (see Material and Methods). We found that MD caused a slight but not significant reduction of the angular size of sub- and suprathreshold RFs in L4Ns of mV1 (PSP-RFs: 89.1 ± 7.7° vs. 67.7 ± 8.4°; medians of AP-RFs: 34.7° vs. 20.4°; data not shown, $P > 0.05$). Similarly, we failed to find a consistent effect of MD on the angular size of RFs in L4Ns of bV1 (PSP-RFs: 55.9 ± 4.3° vs. 61.4 ± 5.4°; medians of AP-RFs: 22.1° vs. 19.6°). MD in mV1 did not cause significant

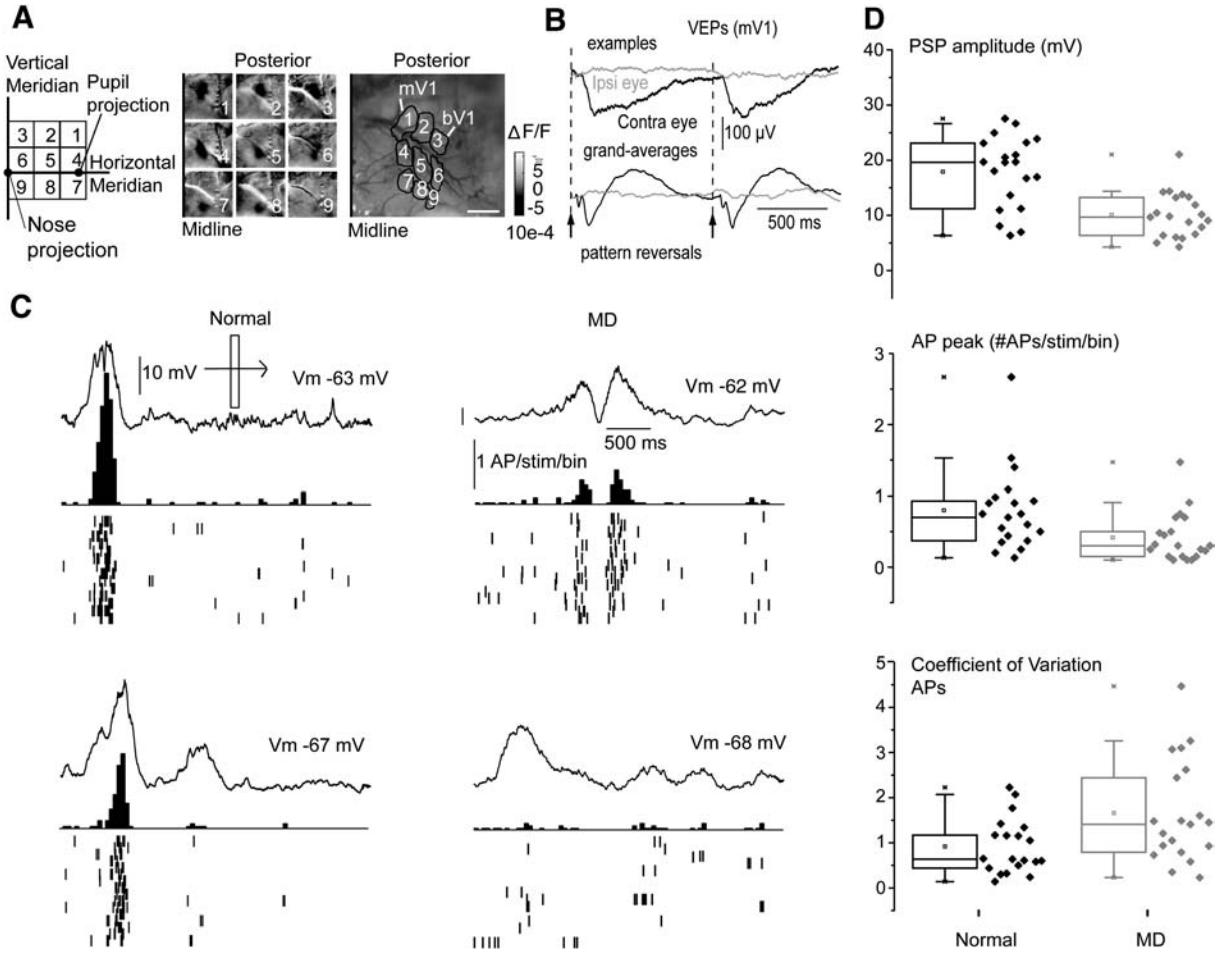


**Figure 4.** MD reduced sub- and suprathreshold visual responsiveness of L4Ns in mV1. (*A*) mV1 was identified by means of ISI. 20° × 20° spots were presented to the contralateral eye in the visual field positions shown on the left sketch. The corresponding ISI spots (middle) were overlaid with the green vasculature image (right). Craniotomies were then opened in correspondence of the spot positions number 3 and 1 for recordings in bV1 and mV1, respectively. Bar: 1 mm. (*B*) Example (top) and grand average (bottom) of VEP responses showing lack of VEP responses in mV1 to stationary gratings alternating at 0.5 Hz upon ipsilateral eye stimulation (gray). (*C*) Examples of sub- and suprathreshold (PSTH) responses of L4Ns recorded in mV1 in normal and long-term MD rats to contralateral (deprived) eye stimulation. Note the reduced amplitude of subthreshold responses in MD rats. (*D*) Top: MD decreases the amplitude of PSP responses of L4Ns in mV1 upon MD compared with normal rats (*t*-test, $P < 0.001$). Middle: MD reduces the peak amplitude of AP responses of L4Ns in mV1 (Mann–Whitney rank sum test, $P = 0.01$). Bottom: MD causes a reduction of reliability of visually driven spiking, as expressed by a significant increase in the median of the coefficients of variation of visually driven spike counts on a trial-to-trial basis (Mann–Whitney rank sum test, $P < 0.05$).

changes in resting $V_m$, spontaneous AP rates, and cell excitability as measured by AP threshold and cell input resistance (Table 1). Thus, MD causes a comparable degradation of visual responsiveness in L4Ns of mV1 and bV1 at both PSP and AP level, in the absence of modifications of spontaneous activity.

### *Brief MD Depressed Deprived-Eye Inputs in bV1 But Not in mV1*

Extracellular recordings (Mioche and Singer 1989; Frenkel and Bear 2004) as well as calcium imaging (Mrsic-Flogel et al. 2007) documented that in bV1, depression of responsiveness to the deprived eye precedes potentiation of open-eye responses. Our in vivo whole-cell recordings confirmed this result at the level of both PSPs and APs in L4Ns in bV1. Indeed, a brief MD episode (48 h of MD) was enough to cause a significant depression of responsiveness through the contralateral deprived-eye stimulation ($n = 12$ cells; Fig. 5*A*, right; PSPs: 17.1 ± 1.1 vs. 12.3 ± 1.3 mV; *t*-test, $P < 0.05$; medians for APs: 0.94 vs. 0.55 APs/stim/bin; Mann–Whitney rank sum test, $P < 0.05$), whereas no sign of potentiation of ipsilateral open-eye responses was observed (Fig. 5*A*, left; PSPs: 11.2 ± 1.0 vs. 11.2 ± 1.6 mV; *t*-test, $P = 0.97$; medians for APs: 0.44 vs. 0.35 APs/stim/bin; Mann–Whitney rank sum test, $P = 0.7$).

Modeling homosynaptic plasticity foresees a slower pace of experience-dependent depression of responsiveness to a deprived sensory input in the absence of competition (Blais et al. 1999). Thus, we tested whether brief MD, which relies on rather different mechanics compared with long-term MD in bV1 (Gandhi et al. 2008; Yazaki-Sugiyama et al. 2009), was also able to depress synaptic responsiveness in L4Ns of mV1. Whole-cell recordings indicated that this was not the case. Indeed, the amplitude of both PSP and AP visually driven responses was comparable to those of normal rats in L4Ns of mV1 (Fig. 5*B*; $n =$ 19 cells from 10 animals; PSPs: 17.8 ± 1.5 vs. 18.8 ± 1.2 mV; *t*-test, $P = 0.6$; medians for APs: 0.71 vs. 0.95 for control and short-term MD rats, respectively; Mann–Whitney rank sum test, $P = 0.1$). This occurred in the absence of changes of resting $V_m$ values (−69.9 ± 1.6 vs. −71.2 ± 1.8 mV for controls and short-term MD rats,

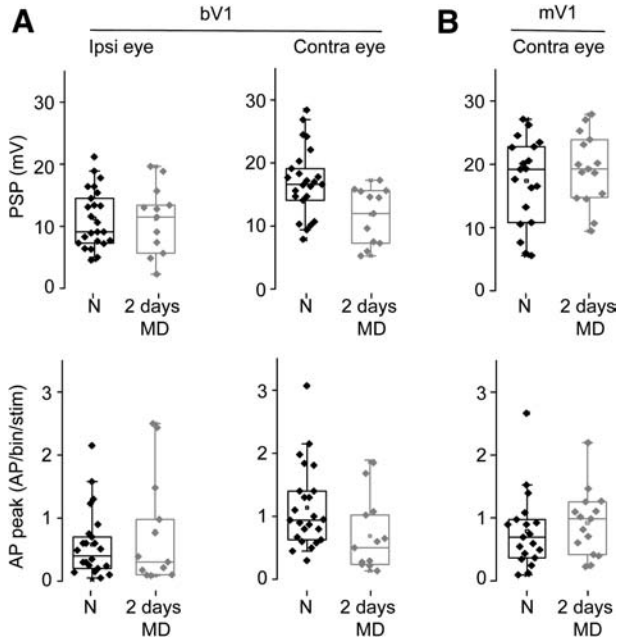


**Figure 5.** A brief MD episode depressed visually driven synaptic responses in bV1 but not in mV1. (*A*) In bV1, 2 days of MD did not cause potentiation of ipsilateral open-eye responses (left column) at both PSP (top; *t*-test, $P = 0.97$) and AP level (bottom; Mann–Whitney rank sum test, $P = 0.7$) but were sufficient to significantly depress contralateral deprived-eye responses (right column) for both PSPs (top; *t*-test, $P < 0.05$) and APs (bottom; Mann–Whitney rank sum test, $P < 0.05$). (*B*) The same manipulation did not significantly depress PSP (top; *t*-test, $P = 0.6$) or AP (bottom; Mann–Whitney rank sum test, $P = 0.1$) responses in L4Ns of mV1.

respectively; *t*-test, $P = 0.6$) or spontaneous AP rates (medians are 0.4 APs/s for both experimental groups; Mann–Whitney rank sum test, $P = 0.33$). Overall, these data indicate that, in the presence of competing inputs driven by the left open eye, loss of responsiveness through the deprived eye is faster.

### *Retinal Inactivation Did* Not Depress Synaptic Responsiveness of L4Ns in mV1

The observation that MD can cause a significant depression of visually driven synaptic inputs in the absence of competing afferents is in agreement with the observations made in the bV1 indicating that loss of responsiveness to the deprived eye occurs via a process of homosynaptic depression. This has been suggested by the observation that silencing retinal activity via intravitreal injections of TTX (MI) causes a smaller ocular preference shift compared with MD (Rittenhouse et al. 1999). Furthermore, VEP recordings have subsequently proven that the scarcer effect of MI on the ocular preference is attributable to a selective blockade of experience-dependent depression (Frenkel and Bear 2004). As we have shown that the depression of deprived-eye responses can occur also in the absence of competing inputs, we tested whether MI affected responses of L4Ns in mV1. At this purpose, we subjected rats to MI by means of daily intravitreal TTX injections for 9 days (see Materials and Methods), followed by 48 h of lid suture to allow for TTX washout (see also the sketch of the experimental protocol in Fig. 6*A*). The results showed that MI was not effective in modifying responsiveness of L4Ns in mV1 (9 rats, 19 cells). Indeed, both PSP and AP responses remained comparable to control rats in rats subjected to MI (see Fig. 6*B*; PSPs: 16.4 ± 1.2 vs. 17.8 ± 1.5 mV for MI and control rats, respectively, one-way

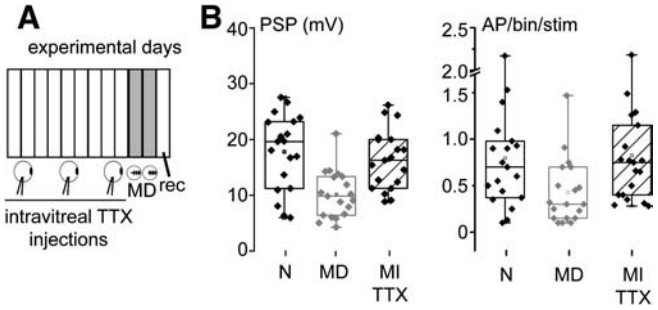


**Figure 6.** Retinal inactivation by intravitreal TTX did not depress PSP and AP visual responses in L4Ns of mV1. (*A*) Sketch of the experimental design for the MI experiment. Animals were subjected to daily intravitreal injections of TTX for 9 days and then to 2 days of MD to allow for TTX washout before electrophysiological recordings. (*B*) Box plots showing the PSP (left) and AP (right) responses of L4Ns in mV1 upon MI. Note that only MD was able to depress sub- and suprathreshold visual responsiveness, whereas MI failed to do so (dashed boxes; PSPs: one-way ANOVA and Tukey post hoc test, $P = 0.7$; APs: ANOVA on ranks, Dunn post hoc test, $P = 0.42$).

ANOVA, Tukey post hoc test, $P = 0.7$; medians for APs: 0.7 vs. 0.75 APs/bin/stim, ANOVA on ranks, Dunn post hoc test, $P = 0.42$). In these animals, resting $V_m$ values were comparable with controls (−69.9 ± 1.6 vs. −70.3 ± 1.4 mV for control and MI rats, respectively; *t*-test, $P = 0.84$) and a slight but nonsignificant increase of spontaneous AP rates was observed (medians: 0.4 vs. 0.7 APs/s, Mann–Whitney rank sum test, $P = 0.07$). These results indicate that, as shown in bV1 (Frenkel and Bear 2004), depression of responsiveness requires the persistence of residual levels of spiking activity from the deprived retina.

### *MD Reduced* Visually Driven Thalamocortical Synaptic Inputs onto L4Ns of mV1

The result that synaptic responses driven by the deprived eye are depressed in the main thalamorecipient lamina of mV1 prompted us to investigate whether MD actually reduces the visually driven thalamic inputs onto L4Ns of mV1, as recently shown in bV1 (Khibnik et al. 2010). To this purpose, we took advantage of an established method to block intracortical synaptic transmission in vivo (Liu et al. 2007; Khibnik et al. 2010), which consists in the intracortical infusion of muscimol+, a cocktail of muscimol and SCH5091 in the appropriate stoichiometry (see Materials and Methods). Muscimol, a γ-aminobutyric acid $(GABA)_A$ receptor agonist, abolishes spiking of cortical neurons, whereas SCH5091, a $GABA_B$ receptor antagonist, leaves intact thalamocortical transmission by preventing the nonspecific activation of presynaptic $GABA_B$ receptors by muscimol. Coupled with VEP recordings in layer 4, this method allowed to demonstrate that MD depresses visually driven thalamic inputs coming from the closed eye in bV1 (Khibnik et al. 2010). Here, we applied the same protocol to measure whether MD actually reduces visually driven thalamic inputs onto L4Ns of mV1. Intracortical infusion of muscimol+ strongly reduced the VEP response to contralateral eye stimulation measured within layer 4 to about one-third within 20 min (musc+ in Fig. 7*A*; reduction to 32.0 ± 3.5%, 7 rats, paired *t*-test, $P < 0.001$; see also Khibnik et al. 2010). As shown in Figure 7*B*, in vivo whole-cell recordings from L4Ns recorded under muscimol+ confirmed a complete silencing of spiking accompanied by the disappearance of spontaneous Up-to-Down state transitions in all recorded cells. The reduction of $V_m$ oscillations reflected in a dramatic decrease of the variance

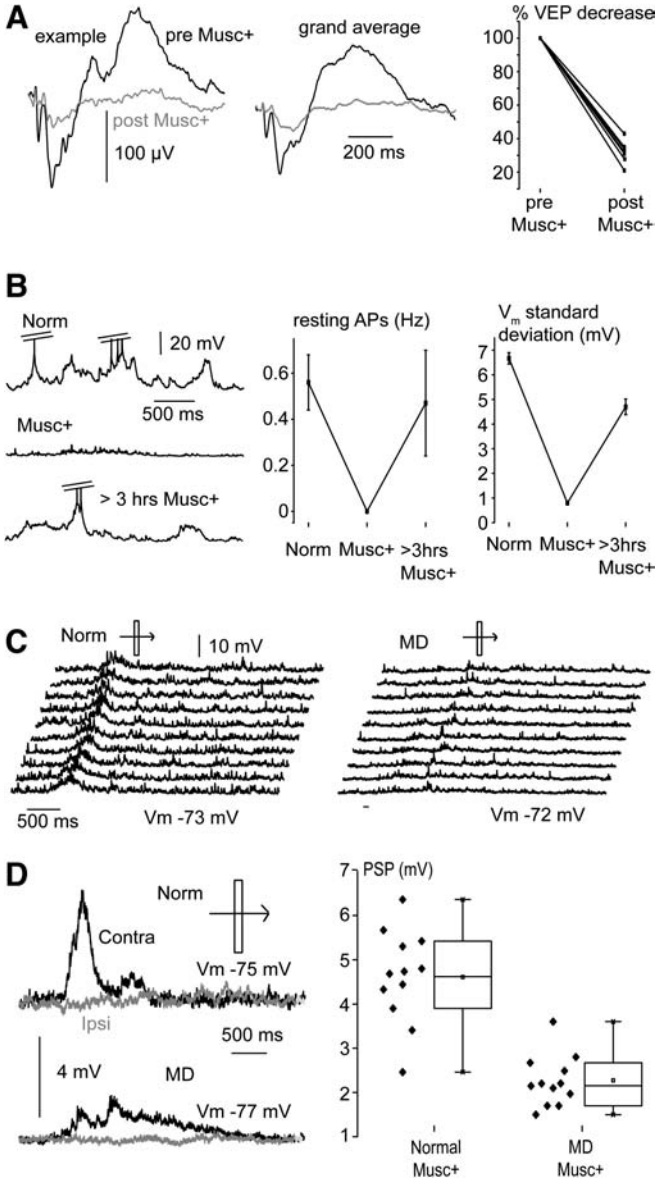


**Figure 7.** MD depresses visually driven thalamic inputs onto L4Ns in mV1. (*A*) Example and grand averages of the VEP responses (left and middle, respectively) recorded in mV1 before (black traces) and after (gray traces) muscimol+ application observed at steady state (Musc+). Note the large decrease in the VEP amplitude after muscimol+ injection, relative to premuscimol+ application (right panel; paired *t*-test, $P < 0.001$). (*B*) Left panel: examples of sub- and suprathreshold activity of intracellularly recorded L4Ns in controls and within 1 h from muscimol+ application (Musc+). After more than 3 h from muscimol+ application, spontaneous activity had recovered to premuscimol+ levels. APs are truncated at −30 mV. Note the complete silencing of AP activity (middle panel) and the disappearance of the large Up-to-Down state subthreshold oscillations (right panel). The amplitude of subthreshold spontaneous oscillations is expressed by the SD of the $V_m$ signal. (*C*) Ten subsequent sweeps showing the subthreshold responses to light bar movement presented to the contralateral eye into 2 L4Ns recorded from a control (left) and an MD (right) rat upon muscimol+ application. Note the marked decrease of the subthreshold responses in the MD rat. (*D*) Subthreshold responses to contralateral eye stimulation of L4Ns recorded in a normal (top) and MD (bottom) rat. Note that ipsilateral eye stimulation did not evoke subthreshold responses, indicating the lack of ipsilaterally driven thalamocortical inputs. Right plot: MD significantly reduced the amplitude of visually driven thalamocortical inputs onto L4Ns of mV1 (*t*-test, $P < 0.001$).

of the $V_m$ over time in absence of visual stimulation (medians are 7.1 vs. 1.0 mV in normal and muscimol-injected rats, respectively; Mann–Whitney rank sum test, $P < 0.001$), in the absence of significant changes of the resting $V_m$ values (–68.6 ± 2.4 vs. –69.6 ± 2.6 mV, *t*-test, $P = 0.8$). In vivo whole-cell recordings were done between 20 and 60 min from muscimol+ application, a time window consistent with the known duration of action of the muscimol+ cocktail (Liu et al. 2007; Khibnik et al. 2010). Indeed, cells patched after 3 h from muscimol+ application, displayed a significant recovery of spiking and subthreshold ongoing activity (Fig. 7*B*, medians for AP rates: 0.24 APs/bin; median for SD of spontaneous $V_m$ oscillations: 4.8 mV; ANOVA on ranks, Dunn's post hoc tests, $P < 0.05$). In all recorded L4Ns of normal rats, low-amplitude depolarizations driven by contralaterally presented visual stimuli were observed (Fig. 7*D*, black; $n = 11$, 4.7 ± 0.4 mV, 27% reduction compared with controls). None of the L4Ns we recorded from mV1 received ipsilaterally driven thalamic inputs (see examples of Figs. 7*C*,*D*, gray). Importantly, the amplitude of visually driven thalamic inputs upon contralateral eye stimulation was significantly smaller for L4Ns recorded from MD rats ($n = 11$) compared with controls (Fig. 7*C*,*D*, right plot; 4.7 ± 0.4 vs. 2.3 ± 0.2 mV; *t*-test, $P < 0.001$). These results indicate that MD reduces the strength of the visually driven thalamocortical drive onto L4Ns of mV1, that is, in the absence of competing inputs from the left open eye. The similarity of the relative decrease of thalamocortical inputs (51%) to that of PSPs (43%) caused by MD in mV1 suggests that loss of feedforward synaptic inputs from thalamic fibers is sufficient to express experience-dependent depression in mV1.

### *BD Degraded Visual Synaptic Responses of L4Ns in bV1*

The data indicate that loss of visually driven synaptic responsiveness in L4Ns can occur in a cortical territory devoid of competing thalamic inputs driven by the left open eye, such as mV1. To confirm that loss of responsiveness can occur independently of competition, we investigated the effects of complete deprivation of patterned vision on sub- and suprathreshold responsivness of L4Ns in bV1. To this aim, a subset of animals was subjected to a period of BD of comparable length (8 rats, 20 cells; see example of visual responses in Fig. 8*A*). BD significantly reduced visually driven synaptic responses to contralateral eye stimulation to a level comparable to MD (Fig. 8*B*, left; Controls: 17.1 ± 1.1, MD: 10.7 ± 0.9, BD: 10.5 ± 1.2 mV; one-way ANOVA, $P < 0.001$; Tukey post hoc test, $P < 0.05$). Ipsilateral eye responses, which are potentiated by MD, were also significantly reduced upon BD (Fig. 8*C*, left; 11.2 ± 1.0 vs. 5.1 ± 0.6 mV; one-way ANOVA, $P < 0.001$; Tukey post hoc test, $P < 0.05$). A similar reduction of visual responsiveness occurred when AP responses driven by the contralateral eye were considered (Fig. 8*B*, right; medians: 0.94 vs. 0.48 APs/bin/stim; one-way ANOVA on ranks, $P < 0.001$; Dunn post hoc test, $P < 0.05$). The same held for ipsilaterally driven AP responses (Fig. 8*C*, right; medians: 0.44 vs. 0.11 APs/bin/stim; one-way ANOVA on ranks, $P < 0.001$; Dunn post hoc test, $P < 0.05$). BD did not modify resting $V_m$ values (–68.7 ± 1.3 vs. –66.2 ± 1.7 mV for control and BD rats, respectively; *t*-test, $P = 0.5$) and only slightly increased spontaneous AP rates (median AP rates: 0.5 vs. 0.8 APs/s; Mann–Whitney rank sum test, $P = 0.08$). Noticeably, the relative strength of the responses of the 2 eyes was not affected by BD, as indicated by the fact that the ODIs were statistically comparable between normal and BD rats for both PSP (Fig. 8*D*, left; ODI-PSPs: 0.21 ± 0.04 vs. 0.34 ± 0.06 for normal and BD rats, respectively; one-way ANOVA and Tukey's

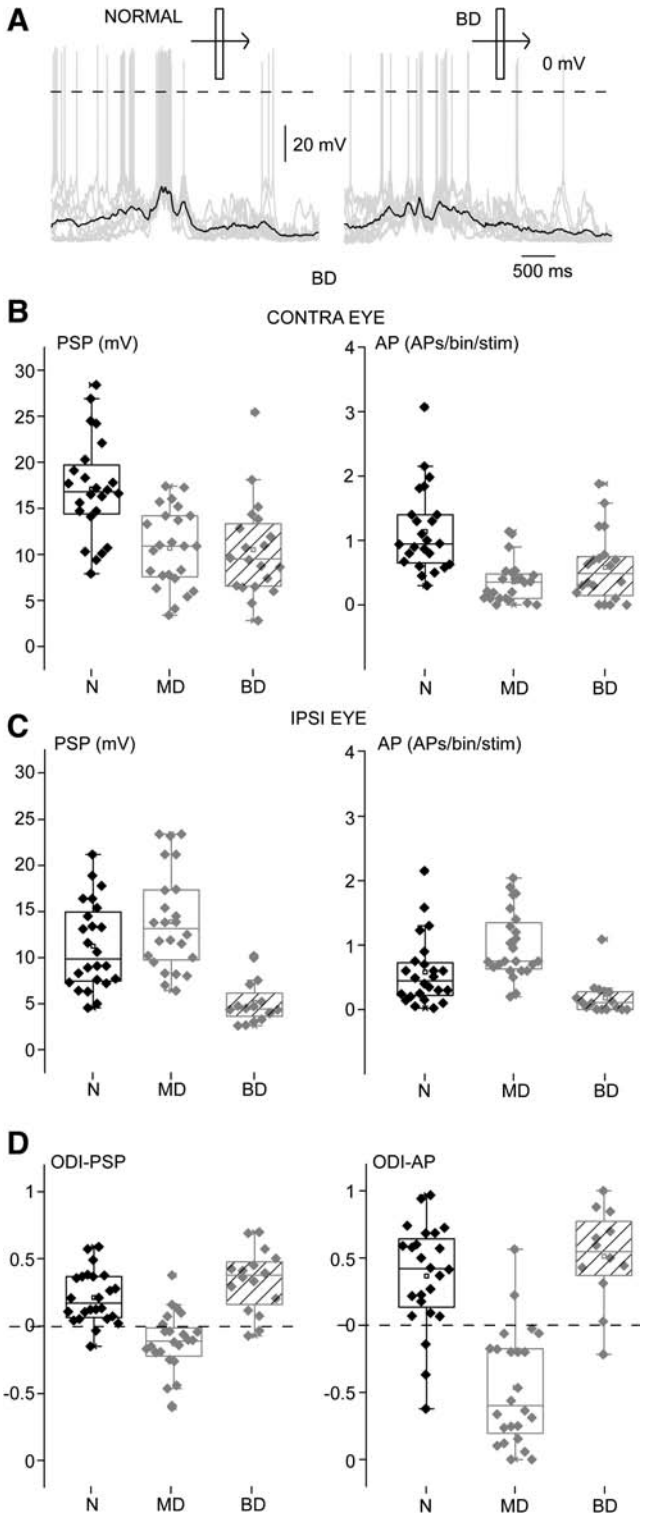


**Figure 8.** BD depressed synaptic and spike responsiveness in L4Ns of bV1. (*A*) Examples of sub- and suprathreshold visual responses to an optimally oriented moving light bar in a L4N recorded from a control (left) and a rat subjected to BD (right). Overlaid sweeps are in gray, the averaged synaptic response—obtained upon AP removal—is in black. (*B*) PSP and AP responses to contralateral eye stimulation in normal (N), MD, and BD rats. BD significantly decreased visual responsiveness at both sub- and suprathreshold level (PSP: one-way ANOVA, $P < 0.001$ and Tukey post hoc test, $P < 0.05$; APs: one-way ANOVA on ranks, $P < 0.001$ and Dunn post hoc test, $P < 0.05$) with respect to controls, and at levels comparable to MD. (*C*) PSP and AP responses to ipsilateral eye stimulation in N, MD, and BD rats. BD significantly decreased visual responsiveness at both sub- and suprathreshold levels (one-way ANOVA on ranks, $P < 0.001$; Dunn post hoc test, $P < 0.05$) with respect to controls and at levels comparable to MD. (*D*) The relative strength of the 2 eyes responses is not affected by MD. The ocular preference of binocular L4Ns, expressed by their ODIs, was significantly modified by MD but not by BD, at both PSP and AP levels (one-way ANOVAs and Tukey post hoc tests, $P > 0.2$).

post hoc test, $P = 0.3$) and AP responses (Fig. 8*D*, right; ODI-APs: 0.37 ± 0.08 vs. 0.51 ± 0.10 for normal and BD rats, respectively; one-way ANOVA and Tukey's post hoc test, $P = 0.2$). BD also shrunk slightly, but significantly, the sub- and suprathreshold RF sizes of visual responses compared with controls (PSP-RFs: 55.9 ± 4.3° vs. 40.5 ± 5.3°, *t*-test, $P < 0.05$; medians of AP-RFs: 34.8° vs. 15.7°, Mann–Whitney *U* test, $P < 0.05$). These data indicate that a complete deprivation of patterned vision during the critical period degrades both sub- and suprathreshold responsiveness in L4Ns of rat bV1.

## Discussion

The ocular preference shift due to long-term MD of L4Ns was sharper at suprathreshold level in bV1, in agreement with the view that the AP threshold renders neurons more selective for the eye that is dominant at subthreshold level (Priebe 2008). At the level of synaptic inputs, loss of responsiveness to the deprived eye was larger compared with the potentiation of inputs from the open eye. The nonlinearities introduced by the AP threshold rendered this difference less pronounced, but still present, at suprathreshold level. Thus, there seems to be a species-specific difference between rats and mice as both VEP recordings (Frenkel and Bear 2004) and in vivo calcium imaging (Mrsic-Flogel et al. 2007; Gandhi et al. 2008) indicate that in mice depression of responsiveness is comparable to potentiation after a saturating period of MD. The larger depression of responsiveness observed in rats is possibly the explanation for the larger ocular dominance shift observed in this species (Fagiolini et al. 1994) compared with mice (Gordon and Stryker 1996). However, it should be stressed that these results are not directly comparable with ours due to the different technical approaches or to layer-specific differences in the plastic response.

We documented a comparable degree of depression of synaptic responsiveness upon long-term MD in L4Ns through the closed eye in both the binocular and monocular subfields of rat V1. Together with the observation that BD reduces visually driven synaptic and spike responses in L4 of bV1, this indicates that a significant loss of subthreshold inputs from a deprived eye can occur in absence of competition from spared active inputs. This is consistent with observations made with extracellular recordings or with imaging techniques. Indeed, complete deprivation of patterned vision during postnatal development degrades responsiveness in V1, as the number of visually unresponsive units is abnormally high in binocularly deprived kittens compared with normal ones (Wiesel and Hubel 1965). In that study, another third of cells were poorly or abnormally responsive, with broader than normal orientation tuning. Similar detrimental effects have been found in kittens experiencing just a few days of dark rearing during the critical period (Freeman et al. 1981), and degradation of AP responses upon dark rearing has been described in rat V1 as well (Fagiolini et al. 1994). Also, ISI showed a comparable loss of visual responsiveness upon MD and BD in mouse bV1 (Faguet

et al. 2009). However, extracellular recordings reported only a slight depression of responsiveness in bV1 of mice binocularly deprived during the critical period (Gordon and Stryker 1996; Frenkel and Bear 2004). Importantly, the effects of MD in mV1 remained controversial. VEPs intracortical recordings (Smith et al. 2009), flavoprotein intrinsic imaging (Tohmi et al. 2006), and functional anatomy with c-fos staining (Pham et al. 2004) revealed that MD is ineffective in mV1. Conversely, ISI (Kaneko et al. 2008; Faguet et al. 2009), epidural VEPs (Heynen et al. 2003), and extracellular spike recordings (Spolidoro et al. 2011) reported a significant depression of responsiveness upon critical period MD in mouse mV1. In some of these reports (Kaneko et al. 2008; Spolidoro et al. 2011), the loss of responsiveness in mV1 was only temporarily observed upon brief MD and not after prolonged MD (but see Faguet et al. 2009). It is difficult to reconcile these findings and compare them with ours mainly for technical reasons. Indeed, c-fos activation and intrinsic imaging only indirectly reflect the spiking activity and even more indirectly the synaptic inputs of V1 neurons. On the other side, the VEPs signal could integrate the dendritic activity of cells located in different layers or of distinct cell types (Katzner et al. 2009), which can exhibit different plastic responses (Gandhi et al. 2008). Finally, extracellular unit recordings are biased toward highly spiking cells and cannot identify the recorded cell types or provide direct information on incoming synaptic inputs. In line with the possibility of layer-specific and cell type–specific effects of complete visual deprivations is the demonstration that these sensory manipulations increase AP responses in supragranular layers (Mrsic-Flogel et al. 2007), an observation we confirmed at the level of synaptic inputs (G Iurilli and P Medini, unpublished data). In addition, recent slice works indicated that MD during the critical period causes layer-specific changes in excitability in pyramidal neurons of mV1, which is increased in supragranular layers (Maffei and Turrigiano 2008) but decreased in infragranular layers (Nataraj et al. 2010). The presence of layer-specific and cell type–specific differences in the response to complete visual deprivations in V1 could partially account for the controversial results in the literature. However, the possibility of species-specific differences (mouse vs. rat) cannot be excluded. In vivo whole-cell recordings from the distinct cell types composing vertical microcircuits will help discriminating these possibilities.

Mechanistically, our results are consistent with the view that a process of homosynaptic depression mediates loss of responsiveness upon visual deprivation. This has been initially suggested by the discovery that MI causes a smaller ocular preference shift compared with MD in kittens (Rittenhouse et al. 1999). This occurs because MI selectively prevents the depression of closed-eye responses upon MD (Frenkel and Bear 2004) and is accompanied by an increase of the spiking correlation among thalamic units (Linden et al. 2009). Our result that MI is not effective in depressing synaptic responsiveness in mV1 corroborates the hypothesis that the loss of visual responsiveness to the deprived eye in mV1 is driven by a homosynaptic LTD-like process. Second, the fact that the decrease of thalamocortical inputs is proportional to the decrease of subthreshold visual responses suggests that loss of responsiveness in mV1 is primarily due to loss of strength of visually driven thalamocortical inputs onto L4Ns, as described in bV1 with VEPs (Khibnik et al. 2010). The main difference we found with respect to MD effects in bV1 is that experience-dependent loss of visual responsiveness is slower in mV1. Indeed, 2 days of MD, which are effective in depressing visual responses in bV1 (see also Mioche and Singer 1989; Frenkel and Bear 2004; Mrsic-Flogel et al. 2007), did not cause a similar effect in mV1. This indicates that the presence of visually driven competing inputs coming from the left open eye accelerates the process of homosynaptic depression of closed-eye inputs. The most parsimonious interpretation is that in bV1, visually driven firing—due to open-eye activity—decorrelates the AP activity of the cell with respect to closed-eye inputs, thus contributing to faster depression of the latter. The results are in agreement with homosynaptic models of MD-driven plasticity, which foresee that loss of responsiveness is faster in the presence of competing inputs (Blais et al. 1999).

Which could be the possible molecular mechanisms underlying the competition-independent loss of responsiveness we documented in mV1? First, internalization of GluR1 2-amino-3-(5-methyl-3-oxo-1,2- oxazol-4-yl)propanoic acid receptors, which in bV1 is driven by MD (Heynen et al. 2003) and is required for the expression of ocular dominance plasticity (Yoon et al. 2009), occurs in mV1 as well (Heynen et al. 2003). Second, during the critical period, MD selectively potentiates inhibitory transmission between fast-spiking basket cells and L4Ns in both mV1 (Maffei et al. 2006) and bV1 (Maffei et al. 2010), suggesting that potentiation of visually driven inhibition could underlie the observed loss of responsiveness, either by reducing the evoked response or by triggering the depression of thalamocortical synapses (Khibnik et al. 2010, reviewed in Smith and Bear (2010)). It has to be stressed that the lack of significant modifications of spontaneous activity or cell excitability we observed upon complete visual deprivations does not exclude homeostatic plasticity (e.g., of visually driven inhibition) that could underlie the observed effects. Future work will clarify the differential role of these mechanisms in competition-independent synaptic plasticity in the visual cortex.

A comparison with the other widely used system to study experience-dependent plasticity in rodents—the somatosensory (barrel) cortex—indicates that both complete unilateral (Glazewski et al. 1998; Popescu and Ebner 2010) and bilateral (Popescu and Ebner 2010) whisker trimming degrade spiking responses in layer 4 barrel neurons, albeit in the first case depression is greater if some active inputs remain (Glazewski et al. 1998). Taken together, these and our observations suggest that depression of responsiveness driven by complete sensory deprivations in the main thalamorecipient lamina may be of general relevance in primary sensory cortices.


## Funding

Compagnia San Paolo Programma Neuroscienze (grant to P.M.).

## Notes

We are grateful to Carlo Orsini, Giacomo Pruzzo, and Alessandro Parodi for excellent technical assistance and Jacopo-Giordano Venturoli for performing part of the histochemical reactions. Author Contribution: G.I. did the electrophysiological experiments and analyzed data; P.M. did some of the experiments, designed the experiments, analyzed the data, and wrote the manuscript with F.B. *Conflict of Interest* : None declared.


## References


Blais BS, Shouval HZ, Cooper LN. 1999. The role of presynaptic activity in monocular deprivation: comparison of homosynaptic and heterosynaptic mechanisms. Proc Natl Acad Sci U S A. 96:1083–1087.

Brecht M, Roth A, Sakmann B. 2003. Dynamic receptive fields of reconstructed pyramidal cells in layers 3 and 2 of rat somatosensory barrel cortex. J Physiol. 553:243–265.
Brecht M, Sakmann B. 2002. Dynamic representation of whisker deflection by synaptic potentials in spiny stellate and pyramidal cells in the barrels and septa of layer 4 rat somatosensory cortex. J Physiol. 543:49–70.
Caleo M, Lodovichi C, Maffei L. 1999. Effects of nerve growth factor on visual cortical plasticity require afferent electrical activity. Eur J Neurosci. 11:2979–2984.
Chadderton P, Agapiou JP, McAlpine D, Margrie TW. 2009. The synaptic representation of sound source location in auditory cortex. J Neurosci. 29:14127–14135.
Coleman JE, Nahmani M, Gavornik JP, Haslinger R, Heynen AJ, Erisir A, Bear MF. 2010. Rapid structural remodeling of thalamocortical synapses parallels experience-dependent functional plasticity in mouse primary visual cortex. J Neurosci. 30:9670–9682.
Constantinople CM, Bruno RM. 2011. Effects and mechanisms of wakefulness on local cortical networks. Neuron. 69:1061–1068.
Fagiolini M, Pizzorusso T, Berardi N, Domenici L, Maffei L. 1994. Functional postnatal development of the rat primary visual cortex and the role of visual experience: dark rearing and monocular deprivation. Vision Res. 34:709–720.
Faguet J, Maranhao B, Smith SL, Trachtenberg JT. 2009. Ipsilateral eye cortical maps are uniquely sensitive to binocular plasticity. J Neurophysiol. 101:855–861.
Freeman RD, Mallach R, Hartley S. 1981. Responsivity of normal kitten striate cortex deteriorates after brief binocular deprivation. J Neurophysiol. 45:1074–1084.
Frenkel MY, Bear MF. 2004. How monocular deprivation shifts ocular dominance in visual cortex of young mice. Neuron. 44:917–923.
Gandhi SP, Yanagawa Y, Stryker MP. 2008. Delayed plasticity of inhibitory neurons in developing visual cortex. Proc Natl Acad Sci U S A. 105:16797–16802.
Gentet LJ, Avermann M, Matyas F, Staiger JF, Petersen CC. 2010. Membrane potential dynamics of GABAergic neurons in the barrel cortex of behaving mice. Neuron. 65:422–435.
Glazewski S, McKenna M, Jacquin M, Fox K. 1998. Experience-dependent depression of vibrissae responses in adolescent rat barrel cortex. Eur J Neurosci. 10:2107–2116.
Gordon JA, Stryker MP. 1996. Experience-dependent plasticity of binocular responses in the primary visual cortex of the mouse. J Neurosci. 16:3274–3286.
Heynen AJ, Yoon BJ, Liu CH, Chung HJ, Huganir RL, Bear MF. 2003. Molecular mechanism for loss of visual cortical responsiveness following brief monocular deprivation. Nat Neurosci. 6:854–862.
Kaneko M, Stellwagen D, Malenka RC, Stryker MP. 2008. Tumor necrosis factor-alpha mediates one component of competitive, experience-dependent plasticity in developing visual cortex. Neuron. 58:673–680.
Katzner S, Nauhaus I, Benucci A, Bonin V, Ringach DL, Carandini M. 2009. Local origin of field potentials in visual cortex. Neuron. 61:35–41.
Khibnik LA, Cho KK, Bear MF. 2010. Relative contribution of feedforward excitatory connections to expression of ocular dominance plasticity in layer 4 of visual cortex. Neuron. 66:493–500.
Linden ML, Heynen AJ, Haslinger RH, Bear MF. 2009. Thalamic activity that drives visual cortical plasticity. Nat Neurosci. 12:390–392.
Liu BH, Wu GK, Arbuckle R, Tao HW, Zhang LI. 2007. Defining cortical frequency tuning with recurrent excitatory circuitry. Nat Neurosci. 10:1594–1600.
Maffei A, Lambo ME, Turrigiano GG. 2010. Critical period for inhibitory plasticity in rodent binocular V1. J Neurosci. 30:3304–3309.
Maffei A, Nataraj K, Nelson SB, Turrigiano GG. 2006. Potentiation of cortical inhibition by visual deprivation. Nature. 443:81–84.
Maffei A, Turrigiano GG. 2008. Multiple modes of network homeostasis in visual cortical layer 2/3. J Neurosci. 28:4377–4384.
Margrie TW, Meyer AH, Caputi A, Monyer H, Hasan MT, Schaefer AT, Denk W, Brecht M. 2003. Targeted whole-cell recordings in the mammalian brain in vivo. Neuron. 39:911–918.
Mioche L, Singer W. 1989. Chronic recordings from single sites of kitten striate cortex during experience-dependent modifications of receptive-field properties. J Neurophysiol. 62:185–197.
Mrsic-Flogel TD, Hofer SB, Ohki K, Reid RC, Bonhoeffer T, Hubener M. 2007. Homeostatic regulation of eye-specific responses in visual cortex during ocular dominance plasticity. Neuron. 54:961–972.
Nataraj K, Le Roux N, Nahmani M, Lefort S, Turrigiano G. 2010. Visual deprivation suppresses L5 pyramidal neuron excitability by preventing the induction of intrinsic plasticity. Neuron. 68:750–762.
Peters A, Kara DA, Harriman KM. 1985. The neuronal composition of area 17 of rat visual cortex. III. Numerical considerations. J Comp Neurol. 238:263–274.
Pham TA, Graham SJ, Suzuki S, Barco A, Kandel ER, Gordon B, Lickey ME. 2004. A semi-persistent adult ocular dominance plasticity in visual cortex is stabilized by activated CREB. Learn Mem. 11:738–747.
Pizzorusso T, Medini P, Berardi N, Chierzi S, Fawcett JW, Maffei L. 2002. Reactivation of ocular dominance plasticity in the adult visual cortex. Science. 298:1248–1251.
Popescu MV, Ebner FF. 2010. Neonatal sensory deprivation and the development of cortical function: unilateral and bilateral sensory deprivation result in different functional outcomes. J Neurophysiol. 104:98–107.
Priebe NJ. 2008. The relationship between subthreshold and suprathreshold ocular dominance in cat primary visual cortex. J Neurosci. 28:8553–8559.
Restani L, Cerri C, Pietrasanta M, Gianfranceschi L, Maffei L, Caleo M. 2009. Functional masking of deprived eye responses by callosal input during ocular dominance plasticity. Neuron. 64:707–718.
Rittenhouse CD, Shouval HZ, Paradiso MA, Bear MF. 1999. Monocular deprivation induces homosynaptic long-term depression in visual cortex. Nature. 397:347–350.
Smith GB, Bear MF. 2010. Bidirectional ocular dominance plasticity of inhibitory networks: recent advances and unresolved questions. Front Cell Neurosci. 4:21.
Smith GB, Heynen AJ, Bear MF. 2009. Bidirectional synaptic mechanisms of ocular dominance plasticity in visual cortex. Philos Trans R Soc Lond B Biol Sci. 364:357–367.
Spolidoro M, Putignano E, Munafo C, Maffei L, Pizzorusso T. 2011. Inhibition of matrix metalloproteinases prevents the potentiation of nondeprived-eye responses after monocular deprivation in juvenile rats. Cereb Cortex. doi: 10.1093/cercor/bhr158.
Tohmi M, Kitaura H, Komagata S, Kudoh M, Shibuki K. 2006. Enduring critical period plasticity visualized by transcranial flavoprotein imaging in mouse primary visual cortex. J Neurosci. 26:11775–11785.
Tsiola A, Hamzei-Sichani F, Peterlin Z, Yuste R. 2003. Quantitative morphologic classification of layer 5 neurons from mouse primary visual cortex. J Comp Neurol. 461:415–428.
Wiesel TN, Hubel DH. 1965. Comparison of the effects of unilateral and bilateral eye closure on cortical unit responses in kittens. J Neurophysiol. 28:1029–1040.
Wilent WB, Contreras D. 2005. Stimulus-dependent changes in spike threshold enhance feature selectivity in rat barrel cortex neurons. J Neurosci. 25:2983–2991.
Yazaki-Sugiyama Y, Kang S, Cateau H, Fukai T, Hensch TK. 2009. Bidirectional plasticity in fast-spiking GABA circuits by visual experience. Nature. 462:218–221.
Yoon BJ, Smith GB, Heynen AJ, Neve RL, Bear MF. 2009. Essential role for a long-term depression mechanism in ocular dominance plasticity. Proc Natl Acad Sci U S A. 106:9860–9865.
Zilles K, Wree A, Schleicher A, Divac I. 1984. The monocular and binocular subfields of the rat's primary visual cortex: a quantitative morphological approach. J Comp Neurol. 226:391–402.